Journal of Power Sources, *15* (1985) 261 - 285

THE ELECTROCHEMISTRY OF POROUS ZINC V. THE CYCLING BEHAVIOUR OF PLAIN AND POLYMER-BONDED POROUS ELECTRODES IN KOH SOLUTIONS

N A HAMPSON and A J S McNEIL

Department of Chemistry, Loughborough University of Technology, Loughborough, Leicestershire, LE11 3TU (U K)

(Received September 24, 1984, in revised form May 24, 1985)

Summary

A range of novel zinc electrode materials, incorporating simple polymers (poly(styrene), poly(methyl methacrylate), poly(vinyl chloride), poly(isoprene), poly(vinyl acetate) and poly(carbonate)) were prepared via a soluble route After characterising their structures using scanning electron microscopy, the discharge and cycling behaviour was studied. The presence of most polymers, notably poly(styrene) and poly(vinyl chloride), reduced both the proportion of accessible zinc in the electrode and the cycle life, owing to the rigid and constricted polymer matrix becoming blocked with discharge reaction products. Some polymers, such as poly(methyl methacrylate) and poly(vinyl acetate), however, could significantly increase the cycle life at low levels of addition. Poly(carbonate) was exceptional in that it permitted total zinc utilisation, with a greatly increased cycle life, stabilising the zinc electrode structure against shedding. The cycling performance of the polymeric electrode materials can be related to their steady state polarisation behaviour.

1. Introduction

Within the context of long-term cycling behaviour, which is limited by shape change processes, the short-term performance of the zinc anode is limited by passivation. This is marked by a precipitous drop in dissolution current to nearly zero, or, conversely, an increase in potential to that for oxygen evolution, associated with surface coverage by anodic oxidation products. Powers and Breiter [1 - 4] observed two types of anodic product film: type I, white, loose, and formed by precipitation from supersaturated zincate solution; and type II, a compact film formed directly on the surface rather than by precipitation, and which was considered responsible for passivation. These careful observations have become the classical description of the anodic dissolution and passivation of zinc, and have been substan-

0378-7753/85/$3 30

tiated by other workers. The situation is not straightforward, however, and the behaviour of zinc depends upon the precise balance of experimental conditions. McKubre and MacDonald [5] have recently related the results of their rotating disc electrode (RDE) study to the extensive literature available, and have proposed a four-step physical model for the anodic behaviour of zinc, comprising active dissolution, pre-passivation, pseudo-passivation, and finally true passivation. The important pre-passivation stage involves the formation of a thick porous (type I) film of $Zn(OH)_2$ on the electrode from the locally supersaturated zincate solution. Passivation involves the formation of a thin compact (type II) ZnO film due to local depletion of OH^- and diminished pH-value in the porous hydroxide film.

Liu *et al* [6] proposed a similar scheme of sequential reaction steps, after a study of the galvanostatic passivation of static electrodes. This comprised three steps: (1) dissolution and development of a critical zincate concentration, (2) establishment of a porous (type I) ZnO film, and (3) establishment of a compact passivating (type II) film.

The relative times for these steps, however, depend upon the precise experimental conditions. Liu *et al* distinguished a low-current scenario where passivation occurs when the mass transport of OH^- ions through the porous ZnO layer is less than that necessary for the anodic zinc reaction.

With solid electrodes we are dealing with conditions in a bulk solution, albeit adjacent to the electrode surface Thus Hampson *et al* , when studying the sharp active–passive transition for galvanostatic polarisation of solid electrodes, observed much longer times for vertical electrodes [7] than for horizontal ones [8]. Porous electrodes, however, showed only gradual active–passive transitions and similar times in both orientations [9] Here the conditions are different: a small volume of electrolyte is isolated from the bulk and is highly quiescent within the confinement of the pores. Moreover, the electric vector along the length of the pore introduces a highly non-uniform distribution of reaction rates. Thus, various workers have concluded that a large proportion of the electrode may contribute little to the measured current [9 - 12].

The isolation of the pore electrolyte can lead to unexpected effects. For example, Hampson and co-workers found that, whereas a smooth zinc electrode returned to its initial condition if a galvanostatic polarisation run was interrupted [7], a porous electrode would passivate more readily after an interruption [9]. This was attributed to the slow decomposition reaction

$$Zn(OH)_4^{2-} = ZnO + H_2O + 2OH^- \qquad (1)$$

In contrast with solid zinc, there have been few direct observations of the passivation of porous electrodes. Nagy and Bockris [13] measured highly non-uniform current distributions within a porous microelectrode in which the current decreased with penetration into the porous structure. They observed, using scanning electron microscopy (SEM), a very porous oxide film of fine needles, which was likened to the type I film seen on

solid electrodes. To explain the reaction profiles, however, they had to postulate the presence of a compact and resistive type II film underneath the type I. The type I film was uniform throughout the electrode, regardless of depth, current density and amount of charge withdrawn, though this may have been due to their particular experimental arrangement.

In contrast, Szpak and Gabriel [14] constructed a single-pore analogue cell. These authors observed a wide variety of ZnO growth forms, varying with current density and position in the pore, all consistent with the solution-precipitation mechanism, involving nucleation, growth and, finally, coalescence of individual crystallites. Compact thick films, which appeared to fold and crack spontaneously on reaching a thickness of a few tens of nm, could be formed in this way.

Katan *et al* [15] also studied the anodic behaviour of zinc within a single model pore, not only by *post mortem* dissection and SEM observations, but also by *in vivo* optical microscopy. They observed the formation of a compact thin dark film, starting at the pore mouth and rapidly penetrating into it during galvanostatic polarisation. The film appeared to form by precipitation of discrete needle-like growths from solution which coalesced and thickened with time. The extension and thickening of this film was accompanied by a gradual increase in polarisation and catastrophic passivation finally occurred with the formation of free ZnO particles throughout the pore electrolyte. Fresh electrolyte redissolved this massive white precipitate within about 3 s, exposed the dark compact film, and removed the polarisation. Katan *et al* [15] concluded that passivation was neither due to a blocking effect of the bulk precipitate, nor to the formation of a second film, but to the concentration polarisation caused by the complete consumption of OH^- ions with decreased pH. (Marshall and Hampson came to the same conclusion on the basis of linear sweep voltammetry experiments [16]) This behaviour does not appear to conform to the mechanism of passivation by duplex film formation observed on solid zinc [1 - 6], and inferred in porous zinc [13].

While the zinc electrode may fail in the short term by passivation, its long-term cycling life is limited by shape change. The active material is redistributed, moving from the electrode edges towards the centre, with an associated reduction in surface area and loss of capacity. Failure by shape change requires only a minute redistribution of material in each cycle, and so the phenomenon is highly sensitive to a variety of operating parameters, as has been discussed by McBreen and collaborators [17, 18]. To this list must be added the adventitious side-effects of the electrode processes. For example, the minute free zinc particles created by fragmentation of dendrites were considered by Szpak *et al* [19] to contribute to shape change. It seems likely that shape change has no single cause, but a multiplicity of factors will degrade the original state of order of the cycled electrode. Thus, a number of theoretical treatments have been successful in modelling the transient and failure conditions of the cycling electrode.

One of the earlier treatments, due to McBreen [17], proposed a concentration cell generated by non-uniform current distributions observed during charge and discharge. This matched the overall movement of zinc from the electrode periphery towards the centre, as well as accounting for other observations. Various other models have been devised, based on membrane electrolyte pumping [20, 21], the theory of ternary electrolytes [22, 23], and migration in solution [24, 25]. All these theoretical treatments were successful in predicting the behaviour of specially designed cells, although matching the theoretical and experimental systems was not always a straightforward matter [26, 27] Experimental tests of these models could reveal unexpected effects. For example, Liu *et al* [28] could not account for the passivation behaviour of their analogue porous electrode in terms of the Sunu and Bennion model [22], and concluded that passivation may have been caused by the plugging of the open pore mouth by the ZnO-catalysed hydrogen evolution reaction

In addition to modelling exercises there have been other, more pragmatic, studies of shape change, with a continuing interest in polymeric binders. Poly(vinyl alcohol) has been tried [29, 30], but attention has concentrated almost exclusively on poly(tetrafluoroethylene) (PTFE). Charkey found that PTFE improved the mechanical integrity of the electrode and the zinc electrode cycle life in both Zn/AgO [31] and in sealed Ni/Zn cells [32]. Cenek *et al* [33] have found that binding with PTFE and poly(ethylene) enhanced the zinc electrode cycle life, suppressing shape change and dendrite growth. The PTFE was introduced as a suspension and then deformed in subsequent mechanical mixing to bind the electrode particles together. Holze and Maas [34] and Kulcsár *et al* [35] illustrated the types of structure obtained for PTFE-bonded carbon and nickel electrodes, respectively.

No consideration has been given, however, to the many other polymers which can be introduced into the zinc electrode via solution in a non-aqueous solvent. Here we report the preparation, structure and cycling performance of porous zinc electrodes incorporating a number of common polymers. It seemed that the most efficient way to assess the cycling behaviour of these electrode materials was to employ them in an unconstrained format in considerable excess of electrolyte. This technique enabled data on electrode cycling performance to be obtained rapidly.

2. Experimental equipment and procedures

2 1 Equipment

The control of the cell cycling and data logging was performed by means of a microcomputer which was modified to incorporate a real-time clock. A 16-channel, multiplexed (12-bit) analogue-to-digital convertor with a resolution of 1 mV in 2048 mV was also used together with relays for switching the charge–discharge constant-current power supply units

The circuit (shown for one string of cells in series in Fig. 1) was designed following the Lundex principle, where the power supplies are mutually opposed for charge and discharge, and are switched in at the required times. The software for cycling control was capable of operating up to eight strings of cells in series, with up to eight cells in each string, each cell being individually monitored by the multiplexed analogue-to-digital convertor. The software ran cycles of discharge, rest, charge, rest, with electrode potential readings being taken at regular intervals The data were recorded for subsequent analysis and plotting.

A more elaborate cell cycling facility, applying a power profile rather than galvanostatic control, has recently been described by Katz *et al* [36].

2 2 Experimental procedures

Electrodes were prepared from pastes containing zinc dust (Analar, 95% assay), zinc oxide (Analar, 99.5% assay), KOH (Analar), and various characterised polymers. The polymers, mostly supplied by RAPRA*, were (1) poly(styrene) (PS) — RAPRA code PS1, $\bar{M}_N = 103\,000$; (2) poly(methyl methacrylate) (PMA) — RAPRA code PMMA1, $\bar{M}_N = 52\,000$; (3) poly(vinyl chloride) (PVC) — RAPRA code PVC1, $\bar{M}_N = 39\,000$; (4) poly(carbonate) (PC) — RAPRA code PC1, $\bar{M}_N = 15\,000$, (5) poly(vinyl acetate) (PVA) — supplied by BDH, mol. wt. ~ 45 000; and (6) poly(isoprene) (PI) — type 1206 supplied by Petrochim. These polymers were

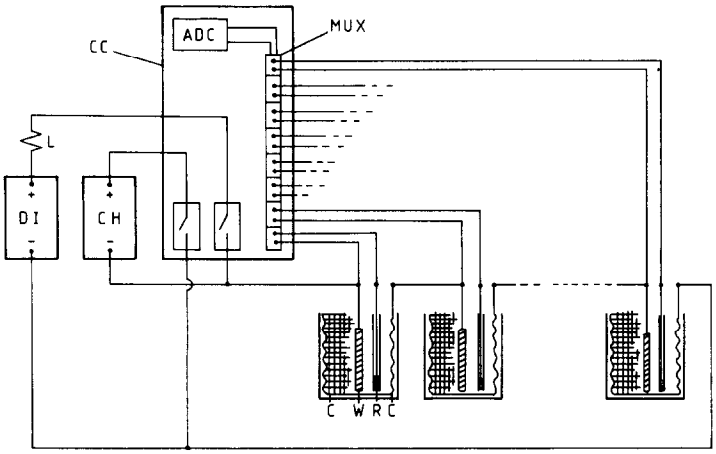

Fig 1 The electrical circuit for controlling and monitoring one string of cells The power supplies DI and CH (the former bearing a dummy load L) are mutually opposed and switched by relays, controlled by the cycle controller (CC), to the string of cells, each cell comprising a working electrode (W) and a reference (R) surrounded by a counter-electrode (C) The multiplex (MUX) switches each cell to the analogue–digital converter (ADC) for the CC to read the zinc electrode potential

*Rubber and Plastics Research Association, Shawbury, Shrewsbury, Shropshire, SY4 4NR, U K

incorporated in the pastes as solutions in tetrahydrofuran (THF, Analar, 0.1% quinol stabilised), except for PC which was dissolved in chloroform, and for PI, dissolved in toluene.

Sufficient polymer solution was added to a dry mix of 50% zinc with 50% zinc oxide to give the required fraction of polymer after total evaporation of the solvent (2%, 10%, 20% or 50% of the dry mix weight). A 50/50 mixture of THF/methanol (or chloroform/methanol for PC, or toluene/methanol for PI) was further added, transforming the rather granular paste to a smooth cream. Earlier experiments [37] had demonstrated that only a small addition of methanol was sufficient to alter the surface condition of zinc dust in THF, and cause this observed change in consistency. The addition of a 50/50 solvent/methanol mixture ensured that both of these volatile liquids were in excess in the paste

Polymer-free zinc pastes were also made up in 0 01 M KOH. In this case the electrodes were prepared immediately, before the zinc could oxidise. It was observed that pastes made up in THF/methanol oxidised only very slowly, and so could be kept for a long time, but this was not so for the Zn/PC pastes.

Zinc electrodes were made up by painting the paste on to a copper gauze current collector (4 cm × 2.5 cm, 40 mesh, degreased, etched in 60% HCl, and thoroughly rinsed). They were built up layer by layer, to reach a weight corresponding to the required discharge capacity (1.35 g of the polymer-free paste, giving 1 A h discharge capacity) and, finally, pressed at a pressure of 1.5×10^8 Pa.

The polymeric pastes generally painted on easily to produce a smooth and uniform electrode. With small polymer additions the dried unpressed electrode was friable, but with an increasing polymer fraction it became strong and even pliable. The exception was PC, with small additions the paste did not paint on smoothly, and though this problem disappeared with larger additions, the paste then tended to crack and peel off the copper gauze during drying, especially with increasing thickness. This was also the behaviour of the PS and PMA pastes made up in THF with no addition of methanol, to such a degree that electrodes could not be fabricated by painting Methanol was thus an essential constituent of these large electrodes. Electrodes made with additions of 50% of PVA and PI were soft and could not be pressed.

The cells were of a very simple design (Fig. 2). The zinc electrode was soldered to a 6BA nickel-plated bolt and suspended from a Perspex jig, alongside an Hg/HgO reference electrode, surrounded by a nickel mesh* counter-electrode (projected area (6 cm × 15 cm), in a 100 ml beaker filled with 90 ml of 7M KOH solution (Analar KOH in tridistilled water). The reference electrode design is shown in Fig. 2; with care in assembly these electrodes were robust and reliable.

*The Expanded Metal Co Ltd , P O Box 14, Longhill Industrial Estate (North), Hartlepool, TS25 1PR, U K

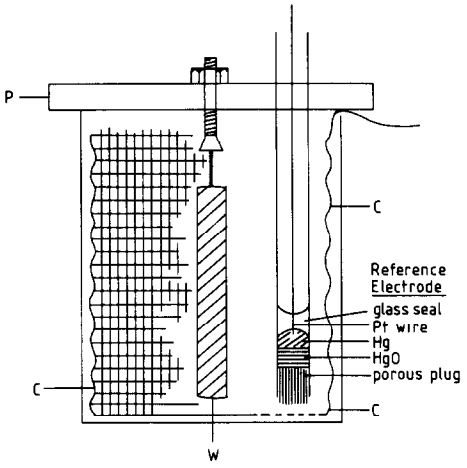

Fig 2 Schematic side view of the cell assembly The working electrode (W) is suspended from the Perspex jig (P), which locates on the 100 ml beaker rim, and is surrounded by the nickel mesh counter-electrode (C), which is shown cut away The reference electrode, also located in the Perspex jig, is 1 5 cm away and normal to one face of the zinc electrode

Electrode charging was at 100 mA, and cycling followed a diurnal period: (1) 7 h discharge at 15 mA; (2) 0.5 h rest; (3) 15 h charge at 8 mA; and (4) 1.5 h rest.

3. Electrode charging and discharging

3 1 Charging

The electrodes were charged at 100 mA (C/4.4 for the 50% Zn/50% ZnO paste) and were given at least 50% overcharge. They were well wrapped in cellulose separator and filter paper to retain their integrity during charging, but were unwrapped for subsequent discharge and cycling tests. This was essential for the plain Zn pastes, but not for the high polymer pastes, which produced very smooth, sound and strong electrodes. Figures 3 and 4 show the potential/time profiles obtained in the reduction of a variety of pastes using values taken at 5 minute intervals. In overcharge, with hydrogen evolution, the zinc electrode potential rose considerably (Fig. 3), as had also been observed with the microelectrodes [38], and could show some fluctuation. In the absence of mercury the hydrogen evolution reaction (HER) was significantly enhanced [39], occurring as a parasitic reaction in cathodic charging, and this could produce aberrations in the apparent electrode charging rate. Prior oxidation of the zinc in the paste was rapid and significant, increasing the amount of charge needed for subsequent reduction. It was noted that, in the absence of mercury, the fully reduced electrodes corroded at the open-circuit potential, with the evolution of hydrogen. The addition of polymer did not noticeably affect

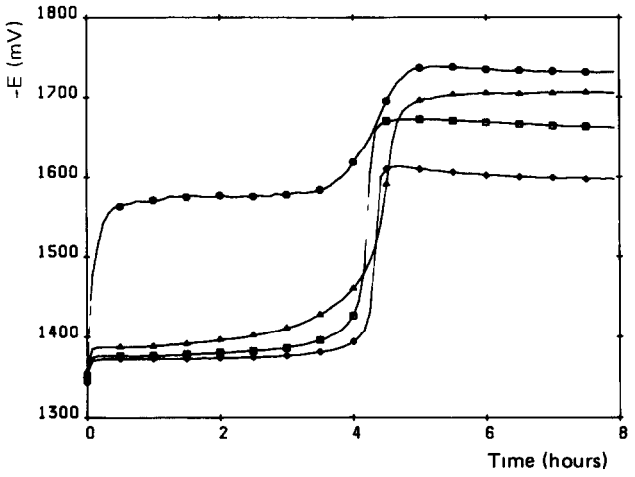

Fig 3 Charging profiles for polymer-free and for Zn/PS electrodes, ♦, Zn(AQ), Zn(THF) and PS2, □, PS10, ▲, PS20, ○, PS50

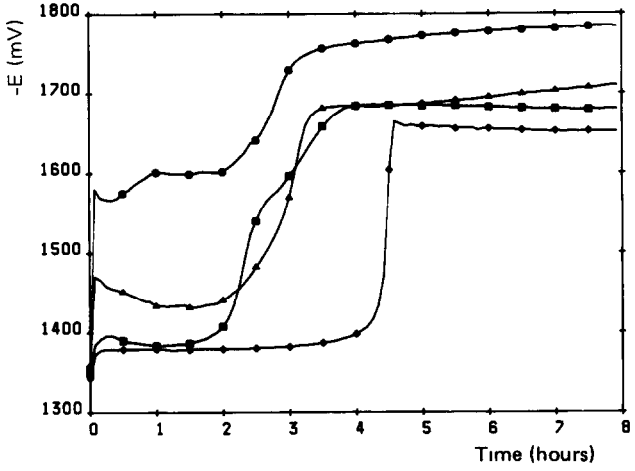

Fig 4 Charging profiles for Zn/PVC electrodes ♦, PVC2, □, PVC10, ▲, PVC20, ○, PVC50

the corrosion rate. The gas bubbles grew to much larger sizes on the polymeric electrodes, however, probably because the aqueous electrolyte could not wet the electrode so readily and dislodge them.

The various polymers incorporated in the zinc pastes affected their behaviour in reduction. Small additions of PS (See Fig. 3), and similarly PMA, did not affect charging behaviour. The PS2 (2% PS) profile was very similar to those for the Zn(AQ) and Zn(THF) electrodes. With increasing polymer concentration, however, first the overcharge potential rose, and then the potential/time profile changed These effects were very likely due to the encapsulation of the zinc oxide particles by the polymer so that

it was more difficult to reduce them, and to drive the reduction reaction into the electrode interior. The influence of PVC upon charging behaviour was very strong, especially at low concentrations (Fig. 4). This polymer also rendered the paste somewhat hydrophobic, so that it was not readily penetrated by the electrolyte, resulting in high initial potential values. In sharp contrast to this pattern of behaviour, the polymer PC had very little effect on the charging profile, and all the PC electrodes resembled the polymer-free electrodes (see Fig. 3) The PC-bonded electrodes appeared to show some instability, revealed by slight discolouration of the electrolyte solution. The PVA50 (50% PVA) electrode displayed extreme behaviour, being very resistant to wetting by the electrolyte solution, so that high potentials were observed in the early stages of charging, even higher than for PVC50 (Fig. 4).

The polymer PI behaved like PS, having minor effects at low concentrations, only decreasing the apparent time needed for full reduction. The PI50 electrode, however, needed a very high potential during the whole of the charging period, and, when the charging current was switched off, could not sustain the normal rest potential.

3 2 Structures of fully charged electrodes

Portions of the freshly charged, uncycled electrodes were prepared for SEM examination by soaking them in methanol for more than 1 hour to remove all KOH, bending to expose the internal structure, and finally applying a 10 nm sputtered gold coating.

The structures of the polymer-free (AQ and THF) electrodes were very similar. Figure 5 shows the wires of the gauze current collector, bearing an active zinc layer which contains pore of a wide size range. The large cavities, up to about a quarter of the size of a grid square, were not present in the dry paste, and must have been produced by hydrogen generated in charging. The zinc was also porous on a microscopic scale (Fig. 6), with the structure comprising zinc granules of various sizes (with hints of facetting) in a continuum of zinc with a fine thread-like morphology. The structure of reduced ZnO contained no granules — these then must be the zinc dust, and the thread-like form must derive from the ZnO. This highly irregular zinc morphology defines a spatially complex void space.

The incorporation of PS profoundly changed this structure (Fig. 7). The polymer had created a rigid three-dimensional mesh which contains the zinc phase. This mesh derives from the polymer solution surrounding the zinc and ZnO particles in the original wet paste. The paste dried with the creation of considerable void fraction (the PS solution occupied five times the volume of the same weight of solid). This structure was deformed in pressing, and then again in fracture. The electron micrograph shows a compacted and distorted, but still recognisable, three-dimensional polymer mesh within which the zinc phase is contained. The zinc morphology is greatly changed with considerable loss of surface area. The zinc granules remain, but the thread-like form is replaced by coarse aggregates, together

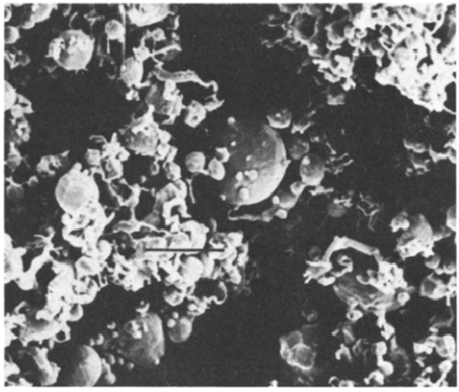

Fig 5 The coarse structure of the Zn(AQ) electrode, lying within the grid of the copper gauze (bar = 100 μm)

Fig 6 The fine bulk structure of the Zn(AQ) electrode In this and subsequent electron micrographs the bar represents 10 μm

with a fine microporous form. The void fraction is less than in plain zinc, and some is isolated within the polymer phase. Such a structure clearly would be more prone to blockage by discharge reaction products. The PS also creates a microporous skin over the electrode, through which small deposits of zinc have grown (Fig. 8).

The PMA produced a skin over the electrode surface very much like the PS. The bulk structure was also similar but more uniform and open. PVC formed a surface skin but this was highly porous and also contained some zinc. PVC was a tenacious elastic polymer, and this shows in the undeformed bulk structure (Fig. 9), clearly deriving from the original disposition of the PVC solution around the zinc and ZnO grains in the wet paste. While this structure is quite open and permeable, the zinc is highly dispersed in small grains

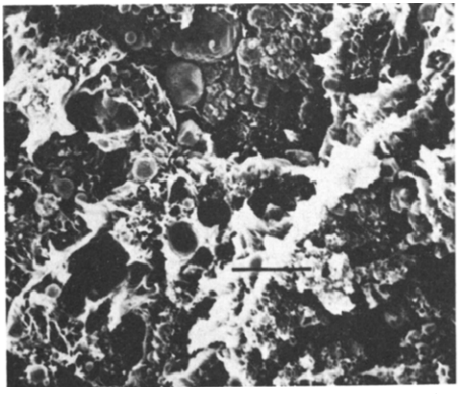

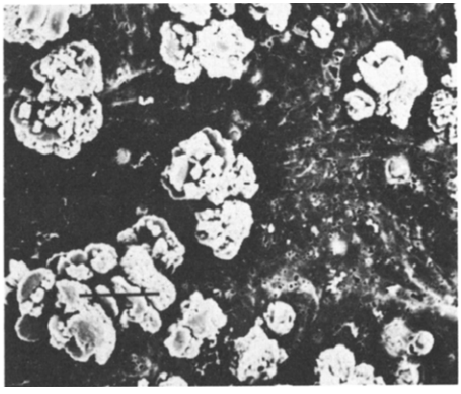

Fig 7 The interior of the PS20 electrode

Fig 8 The free surface of the PS20 electrode

The PC electrodes were very different, with the polymer forming aggregate clumps rather than a tight binding network. This is clearly seen in the electrode surface (Fig. 10), where a fine particulate zinc morphology exists between the clumps of PC, flattened from pressing. The bulk structure (Fig. 11) is very much like that of Zn(AQ), though more dense, with little sign of the PC fraction, probably because the electrode fractured within the weaker zinc phase. This electrode structure was mechanically weak, but the zinc was highly accessible to the solution.

The PVA20 electrode (Fig. 12) shows the familiar network of large polymer cells, within which are the grains of zinc, and also microporous aggregates, derived from ZnO. Figure 13 shows an edge section with the thin permeable polymer skin overlaying the porous bulk structure. The polymer PI behaved very differently from all the others, and acted to wet and encapsulate the zinc rather than form a continuous network (Fig. 14).

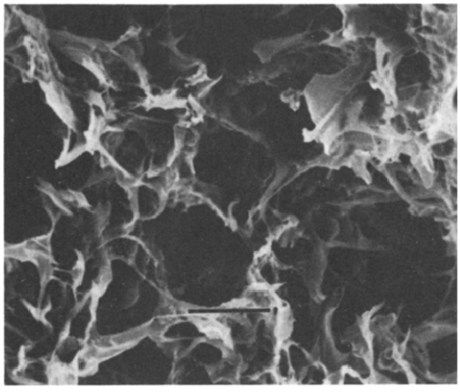

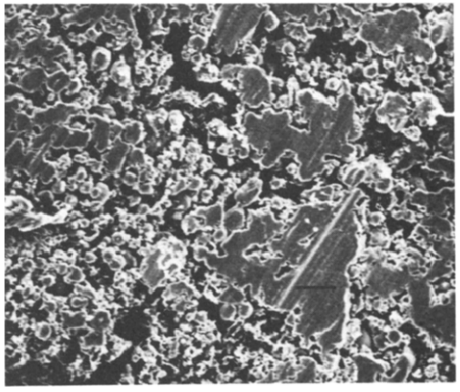

Fig 9 The interior of the PVC20 electrode

Fig 10 The free surface of the PC20 electrode

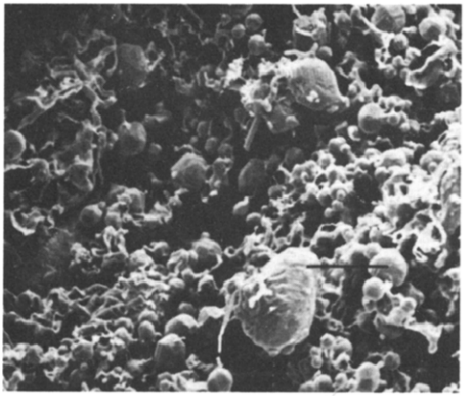

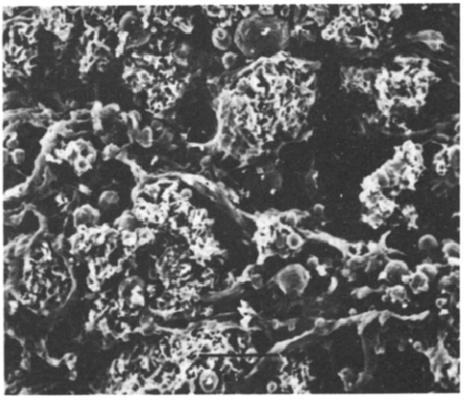

Fig 11 The bulk structure of the PC20 electrode

Fig 12 The bulk structure of the PVA20 electrode

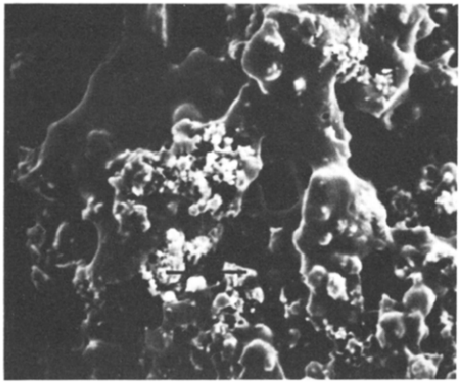

Fig 13 An edge view of the surface of the PVA20 electrode

Fig 14 The bulk structure of the PI20 electrode

The fracture surface, which closely resembled the free surface, showed no sign of deformation because the PI is perfectly elastic. At high percentages the PI is likely to suppress all electrode activity by totally encapsulating the zinc.

3 3 Continuous discharge

As a precursor to the cycling tests, the polymeric electrodes of 1 A h theoretical discharge capacity were tested, unwrapped, in continuous discharge to exhaustion at 15 mA (Figs. 15 and 16). Nearly all polymer additions impaired the ability of the zinc electrode to deliver current and

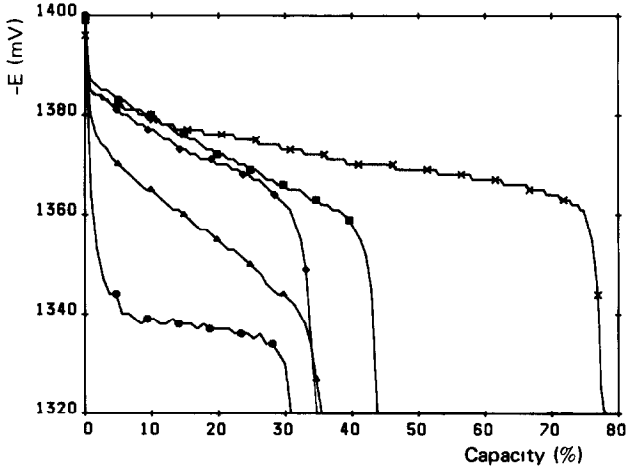

Fig 15 Discharging profiles for polymer-free and Zn/PS electrodes ♦, PS2, ■, PS10, ▲, PS20, ○, PS50, ×, Zn(AQ)

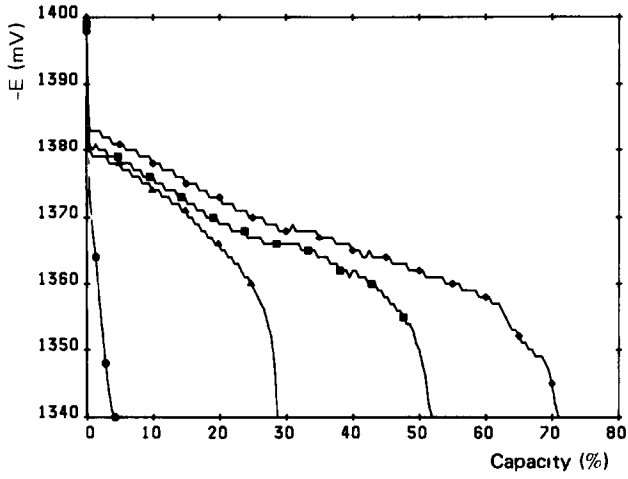

Fig 16 Discharging profiles for Zn/PVA electrodes ♦, PVA2, □, PVA10, ▲, PVA20, ○, PVA50

reduced the total amount of charge which could be withdrawn. Thus for plain zinc and low polymer electrodes (Fig. 15) the potential in discharge remained high, and failure occurred when all the active material had been removed from the copper gauze. The loss of capacity of these electrodes was due mainly to shedding of zinc, observed to occur at large depths of discharge, and also to the parasitic corrosion reaction.

High polymer electrodes tended to show progressive failure, as the remaining zinc, bound up in the polymer matrix within the electrode interior, became increasingly inaccessible for current generation. There could be an optimum polymer level, however, at which zinc shedding was diminished without the discharge reaction being significantly choked.

The combination of these effects is illustrated by the PS electrode series (Fig. 15, also representing the PMA and PVC electrodes), with the 10% electrode affording the best compromise in each case. These polymers severely limited the amount of charge that could be withdrawn from the electrode. The polymers PVA (Fig. 16) and PI were superior in this respect, though at high addition levels they could deliver virtually no current at all. It is the polymer PC that performed best in this test. At all levels it had no harmful effect on current delivery, and made the zinc accessible so as to achieve greater than 80% electrode utilisation (similar to Zn(AQ), Fig. 15).

At the very low discharge rate employed (C/67) there was no passivation of the zinc, and it was totally consumed, as predicted by the calculations of Liu *et al* [6]. In this case the calculations of discharge capacity, based on pore plugging by ZnO, recently made by Chang *et al* [40], do not apply. As the electron micrographs have clearly shown, however, the active zinc could be rendered inaccessible by the polymer additions. The deep discharged polymer-bonded electrodes showed many light grey patches

of ZnO, which were the sites of large hydrogen bubbles (ZnO is known to catalyse hydrogen evolution [2]). Finally, a dark red colour appeared and spread as the copper gauze was oxidised.

The relation between the electrode structure and its discharge capacity was not straightforward. The PI and PVC produced totally different structures which both suppressed the anodic discharge reaction. In the former case the active zinc phase became totally engulfed within the insulating PI. In the latter, the zinc was finely dispersed throughout a continuous polymer mesh, again with electrical isolation and capacity loss. In general, the likely cause of electrode failure is passivation, by blocking of the constricted polymer network with zinc oxide, as envisaged by Sunu and Bennion [23]. This was probably the cause of failure for the PS, PMA and PVA electrodes. In the last case, discharge capacity fell steadily as the polymer content rose. (Fig. 16). The results from electrodes with PC added were notably different. It left the zinc totally accessible for current generation and, consequently, good discharge capacity yet provided some degree of binding.

Two further factors may also contribute to capacity loss. The first is the thin polymer skin formed on some electrodes. The second is the very real possibility of pore blocking by generated hydrogen, which was considered by Liu *et al* [28] in the case of their model pore electrode. The solution would not be able to wet the hydrophobic polymeric structure so readily, and so would not expel the gas phase from the pores.

4. Electrode cycling

4 1 Introduction

The behaviour of each electrode (unwrapped) over its entire cycle life is represented by up to four cycle profiles Each profile shows a common sequence of potential movements resulting from the common cycle of discharge, rest, charge, rest.

4 2 Plain zinc electrodes

The cycling behaviour of the plain zinc electrodes, Zn(AQ) and Zn(THF), was very similar (illustrated by Zn(AQ) in Fig. 17). Both of these electrodes showed a considerable rise in potential during charging in the first cycle (C1). This is an attenuated form of the behaviour seen in Fig. 3 and is due to the onset of hydrogen evolution as the electrolyte is depleted of dissolved zinc. As cycling continued the electrode corroded, the solution zinc concentration steadily rose, and hydrogen evolution soon disappeared.

The rising zinc concentration also produced a positive shift in the free corrosion potential of the zinc electrode, seen at the end of each cycle. The rate of zinc corrosion was not measured, but the data of Gregory *et al* [39] suggest that the loss by displacement of hydrogen could be the equivalent of about 0.004 A h per day. These authors also state that corrosion

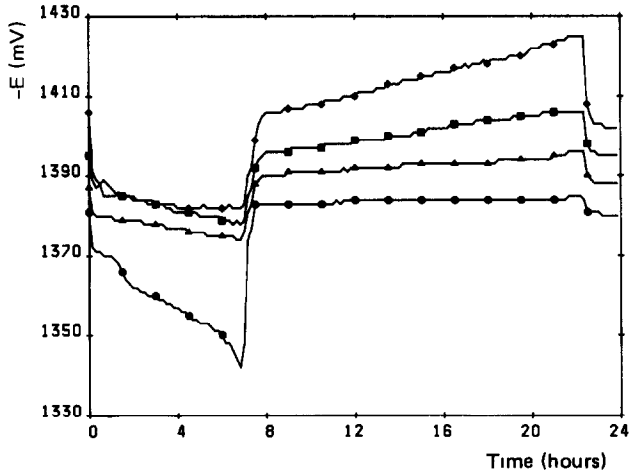

Fig 17 Cycling profiles for the Zn(AQ) electrodes ♦, cycle 1, □, 6, ▲, 10, ○ 15

via the oxygen reduction reaction proceeds faster than via hydrogen evolution. So, in the present work, where both mechanisms operate in air-saturated electrolytes, the total loss of zinc by corrosion may be in the region of 0.01 A h, or 1%, per day.

The electrode quickly developed coarse superficial growths in charging (see Fig. 18). There was a steady migration of zinc over the cycling electrode, to some extent laterally towards the centre, but mostly downwards towards the bottom edge (Fig. 19). This was probably due to the denser

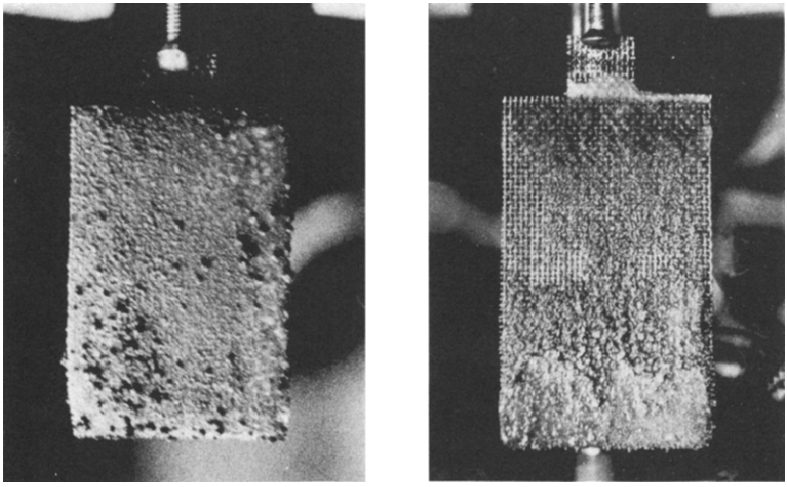

Fig 18 The Zn(AQ) electrode after one cycle, showing small discrete growths built up during the charging phase

Fig 19 The Zn(THF) electrode after eight cycles, illustrating zinc migration, exposure of the gauze, and development of coarse deposits which are periodically shed

zinc-rich solution produced in discharge settling at the bottom of the beaker and then preferentially depositing zinc during charge at the lower end of the electrode. The electrodes thus show the pattern of shape change behaviour observed by McBreen [17], but modified by the presence of a large volume of electrolyte, as McBreen had envisaged.

The mossy growths formed during charging were not able to support their own weight and eventually fell to the bottom of the beaker. This shedding of active material soon took effect and ultimately limited the life of the polymer-free electrodes, which failed when the copper gauze was totally bare. The appearance of a plain zinc electrode after eight cycles (Fig. 19) indicates how rapid this process could be in a large volume of free electrolyte.

4 3 Zinc/poly(styrene) electrodes

The performance of the PS2 and PS10 electrodes was very similar to that of plain zinc (see Fig. 17), but, whereas the plain electrodes only failed upon total zinc loss, the PS electrodes failed when the zinc remaining in the polymer binding became inaccessible. This was probably caused by the constricted pores becoming plugged with discharge products — blockage of the first kind as defined by Sunu and Bennion [23]. Cycling brought about a general transfer of zinc from the interior of the electrode to mossy external growths, which were steadily lost by shedding and corrosion. Figure 20 shows the PS2 electrode at the end of its life, with material clearly remaining on the gauze, but only a small area at the bottom remaining active. The PS10 electrode was wholly "switched off" at the end of its cycle life, and showed light grey patches of ZnO appearing. With further cycling a dull red colour appeared, due to the oxidation of the copper gauze.

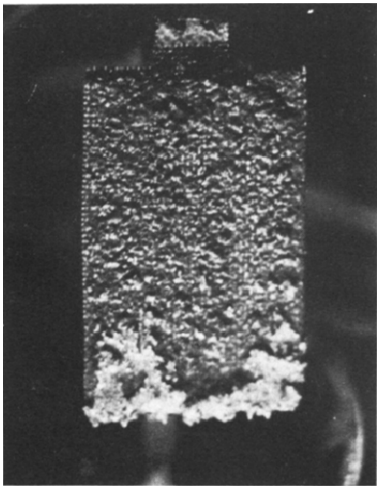

Fig 20 The Zn/PS2 electrode at the end of its life, after 12 cycles, while material remains on the copper gauze only a small fraction of it at the lower end remains active

Increasing the PS level to 20% (Fig. 21) further diminished the electrode's ability to deliver charge, and also introduced a large spike at the start of the charging profile, which shrank as cycling proceeded. This unusual charging behaviour, which we shall refer to as type I, indicates that the electrode had a high resistance at the start of charging that it did not have at the end of discharge. Straightforward explanations invoking zinc depletion or oxide formation during discharge are therefore inadequate This behaviour, however, corresponds to the self-passivation at open-circuit potential seen by Elsdale *et al* [9], and attributed to the slow decomposition of zincate (see reaction (1)). The production of a compact resistive oxide film in the rest period could produce a spike in subsequent charge [11] As the electrode is cycled the transfer of zinc to the exterior means that the self-passivation, and the spike, become less significant.

With the incorporation of 50% PS (Fig. 22) the electrode structure was so constricted that by the fifth cycle (C5) the electrode was clearly passivating during discharge, with rapid polarisation. The C5 profile showed a long delay before the charging potential rose steeply (at ~14 h) to display a spike like that shown by the PS20 electrode We shall refer to this potential arrest in charging, associated with polarisation in discharging, as type II behaviour. It would seem that the ZnO formed during discharge is readily reduced, at the same potential as for the first reduction of the pasted electrode (see Fig 3). The observation of light grey patches on the electrode, even at the end of charge, however, indicated the presence of unreduced ZnO. In earlier cycles the potential arrest in charging was shorter and the subsequent charging behaviour was complicated by the intrusion of hydrogen evolution The two forms of behaviour, type I and type II, displayed by the PS20 and PS50 electrodes, respectively, appeared to be quite distinct, that is, the type I shown by PS20 did not transform to type II with continued cycling.

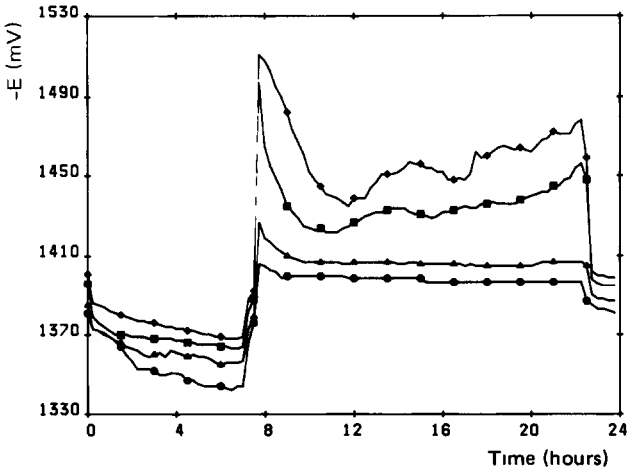

Fig 21 Cycling profiles for the Zn/PS20 electrode ♦, cycle 1, □, 2, ▲, 5, ○7

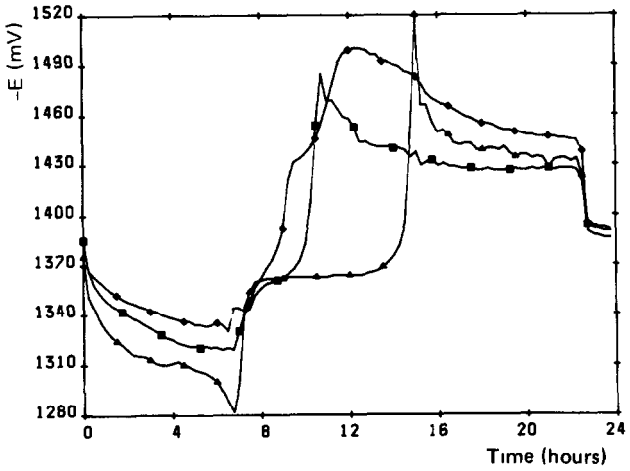

Fig 22 Cycling profiles for the Zn/PS50 electrode ♦, cycle 1, □, 3, ▲, 5

4 4 Zinc/poly(methyl methacrylate) electrodes

The performance of the PMA2 electrode closely resembled that of Zn(AQ) except that it had a much longer cycle life. The PMA maintained nearly uniform coverage of the gauze until the end of the electrode's useful life. The PMA10 electrode showed the charging spike and the accelerated failure more typical of the PS20 electrode. The PMA20 electrode (Fig. 23) shows, in the tenth cycle (C10), how the charging spike is delayed but without any potential arrest at −1360 mV. Figure 24 shows how this electrode was active over only a small fraction of its area, where coarse fragile growths have formed. The PMA50 electrode could deliver virtually no current, and the type II charge arrest, associated with passivation in discharge, appeared in the very first cycle.

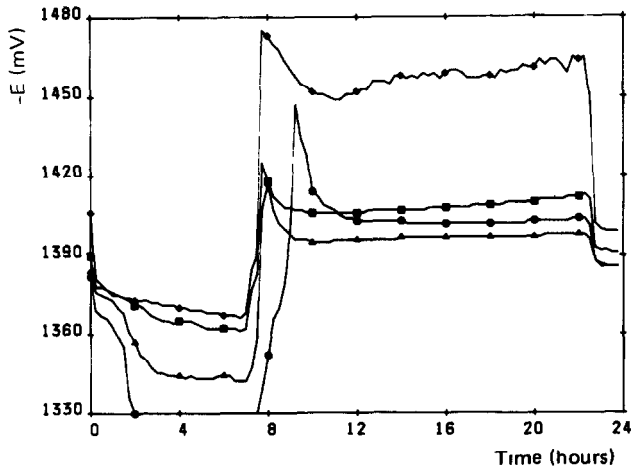

Fig 23 Cycling profiles for the Zn/PMA20 electrode ♦, cycle 1, □, 5, ▲, 9, ○10

4 5 Zinc/poly(vinyl chloride) electrodes

The behaviour of the PVC2 electrode was similar to Zn(AQ), but failed after fifteen cycles. Figure 25 shows how, after 11 cycles, the original smooth surface of this electrode was disrupted by zinc outgrowths formed in charge. The PVC10 electrode had a short cycle life, less than five cycles (Fig. 26) It is interesting that this electrode clearly showed the purely type I behaviour during the first cycle, transforming to the type II. The PVC20 electrode was highly choked and was failing with passivation in the second cycle, rather like PS50 This condition became more extreme in the PVC50

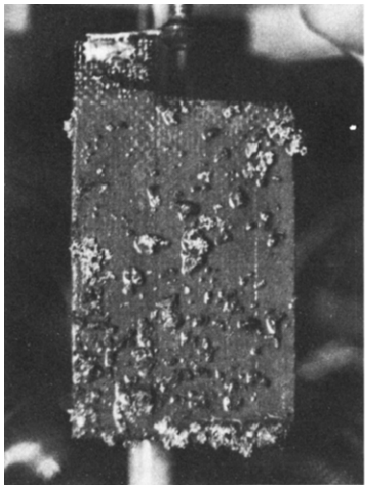

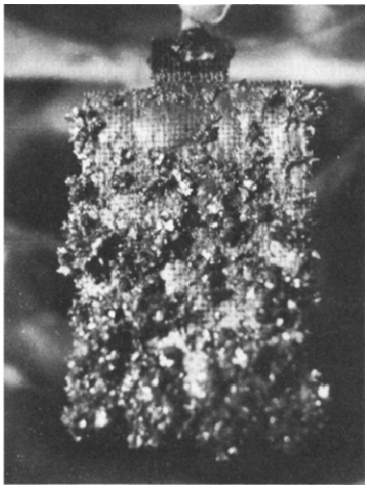

Fig 24 The Zn/PMA20 electrode after eight cycles, showing how most of the electrode had remained smooth and inactive

Fig 25 The Zn/PVC2 electrode after eleven cycles, showing disruption of the originally smooth surface by zinc growths

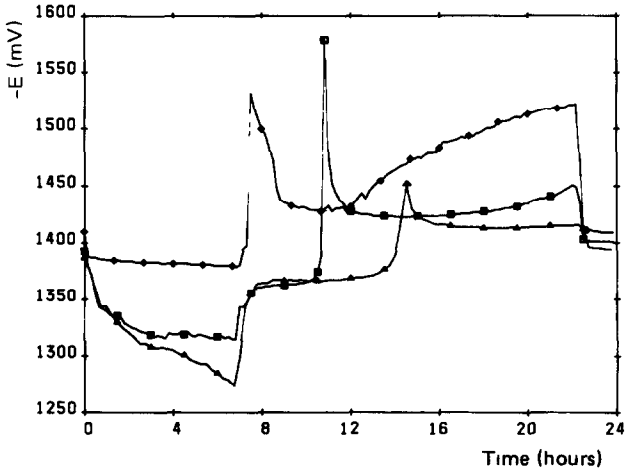

Fig 26 Cycling profiles for the Zn/PVC10 electrode ♦, cycle 1, □, 5, ▲, 9

electrode, so that in cycle nine the electrode reactions appeared to be almost wholly solid state, but this was associated with severe polarisation in discharge.

4 6 Zinc/poly(carbonate) electrodes

In marked contrast to PVC, the incorporation of PC produced highly permeable electrodes, so that at no polymer concentration were any charging spikes seen. The behaviour generally resembles the polymer-free electrodes Rising charging profiles for the early cycles indicate the presence of hydrogen evolution, but even here highly cathodic potentials were not attained. Overall, the PC electrodes were distinguished by very flat cycling profiles and very long cycle lives, even for high polymer electrodes (Fig. 27). The PC2, PC10 and PC20 electrodes behaved much as the Zn(AQ) electrode, the first two failing after 49 cycles, and the PC20 after 22 cycles.

This polymer clearly does not bind and choke the zinc in the same way as PS or PVC, but leaves it available for discharge. Moreover, the deposits formed during charge were more compact, adherent, and resisted shedding (Fig 28). However, the gauze was slowly exposed as the zinc covering slowly shrank down towards the lower end (Fig. 29). The electrodes failed only when the gauze was totally exposed, unlike any of the other polymeric electrodes.

4 7 Zinc/poly(vinyl acetate) electrodes

At low levels (2% and 10%) of PVA the electrode performance was similar to Zn(AQ), but with a cycle life intermediate between the two — 28 cycles for PVA2 The PVA10 electrode still gave a good cycle life, and also showed a charging spike which, unusually, only appeared when the cell was failing. This behaviour was also shown by the PVA20 electrode, which had a much reduced life of eight cycles. Figure 30 shows the good

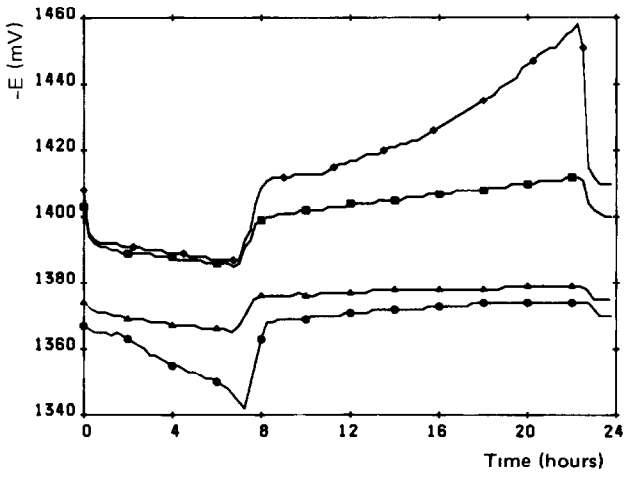

Fig 27 Cycling profiles for the Zn/PC50 electrode ♦, cycle 1, □, 3, ▲, 9, ○, 16

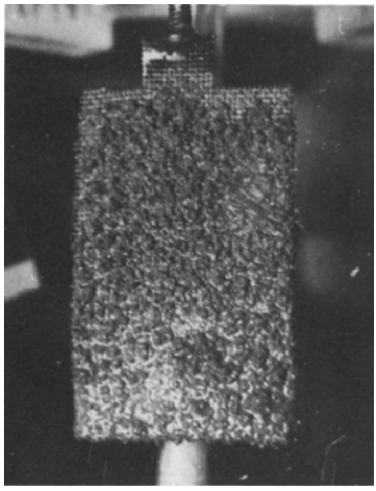

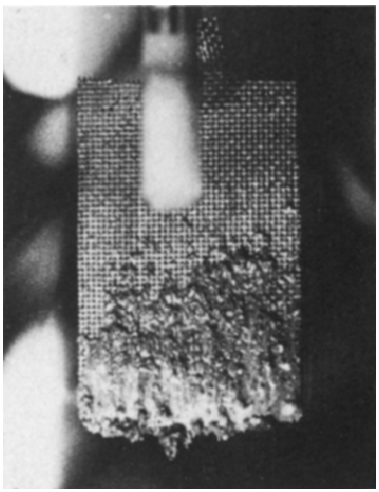

Fig 28 The Zn/PC50 electrode after eleven cycles, showing the development of a compact, adherent deposit

Fig 29 The Zn/PC10 electrode after 40 cycles, showing zinc remaining only on the lower part of the gauze

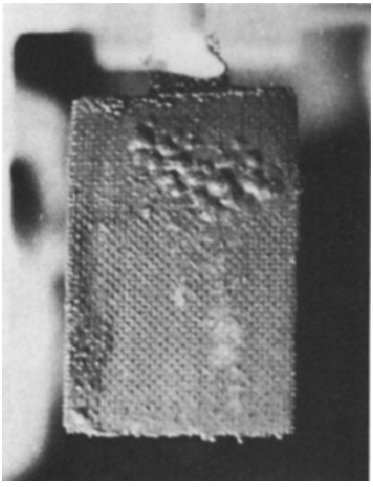

Fig 30 The Zn/PVA10 electrode after 20 cycles, showing smooth uniform coverage, free of external growths

condition of the PVA10 electrode after 20 cycles. In contrast, the failed PVA20 electrode showed large light grey areas indicating extensive ZnO formation. PVA seems to contain the zinc within the electrode very effectively, as shown by the absence of external growths on the cycled electrodes, which had good cycle lives. Too much PVA, however, blocked off the electrode reaction completely. Thus, the PVA50 electrode could not sustain

a discharge potential, and cycling produced the unhealthy condition shown in Fig. 31. The electrode bore large white areas of ZnO, and had also been ruptured by hydrogen generated internally during charging.

4 8 Poly(isoprene) electrodes

The PI2 and PI10 electrodes had long cycle lives and showed the type I charging spike appearing at the point of failure. The PI20 electrode (Fig. 32), with a much shorter life, displayed a spike which shrank with cycling and then grew again as failure approached. It may have been the way the zinc was encapsulated within the insulating PI phase (Fig. 14) that caused the discharge voltage during the first cycle to be less than that for

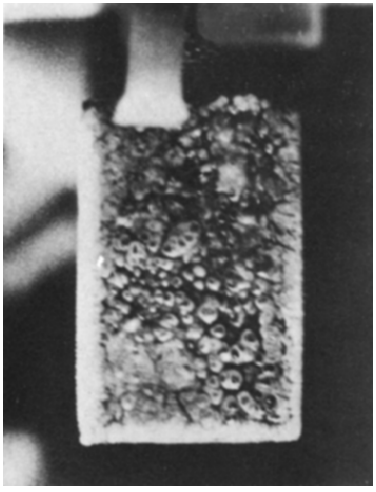

Fig 31 The Zn/PVA50 electrode after 20 cycles, showing large areas of pale ZnO, and blistering due to hydrogen generation

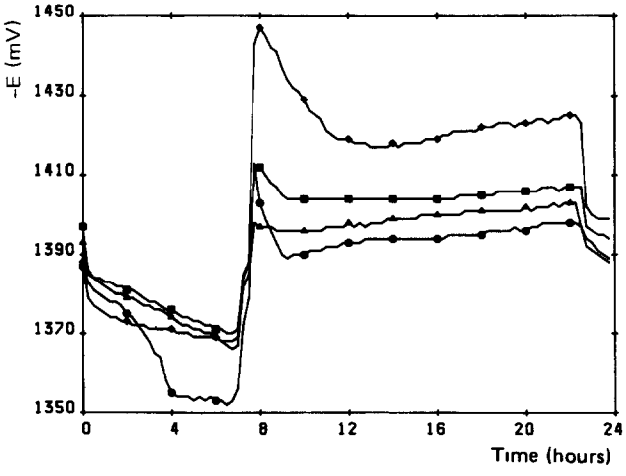

Fig 32 Cycling profiles for the Zn/PI20 electrode ♦, cycle 1, □, 2, ▲, 3, ○, 9

the following two cycles. The PI50 electrode could deliver no current whatsoever, and, considering the structure shown in Fig. 14, it is clear that the active zinc material was totally engulfed by the polymer at this concentration. The PI electrodes, like the PVA series, did not develop surface growths during cycling, and the electrode activity was retained within the electrodes.

5. Electrode cycle life

An electrode's useful cycle life was deemed to have been reached when the discharge potential began to drop sharply, usually corresponding to an end point of about −1350 mV. The cycle lives of all the electrodes are summarised in Fig. 33. The apparent superiority of the Zn(THF) electrodes over the aqueous version cannot on the present evidence, be either fully substantiated or explained. For all of the polymers the cycle life was inversely related to the polymer level. Two polymers, PS and PVC, could not improve on the polymer-free cycle life. The other polymers were able to offer some improvement at low concentrations. The outstanding polymer was PC, offering marked improvement at both low and moderate concentrations.

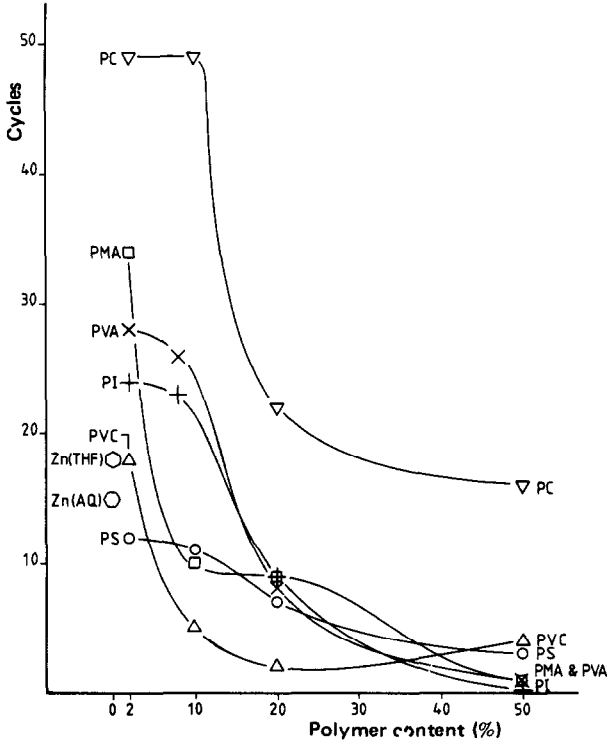

Fig 33 Summary of the cycling performance of all the electrodes tested

The cycling performance of these polymeric electrode materials can be related to their steady state polarisation behaviour, determined using the rotating disc electrode technique [37]. That study found polymer additions fall into two classes, according to their effect on polarisation behaviour and rotation speed dependence of the anodic reaction. The first class of polymers (PC and PI) left the zinc electrode performance more or less unaffected in both respects. The second class (PS, PMA, and PVC) reduced both the anodic current delivered and the rotation speed dependence. PVA was intermediate between the two classes The summary of results in Fig 33 shows that none of the class 2 polymers (with the exception of PMA at the 2% level) could bring any improvement in cycle life. The class 1 polymers, together with PVA, were able to effect significant extensions of cycle life.

6. Conclusions

In this work a novel kind of electrode material, in which the polymer is incorporated by a soluble route, has been studied. The presence of a small amount of methanol was found to be essential in the fabrication of sound electrodes. The incorporation of a polymer generally improved the physical properties of the pasted electrodes, producing smooth, sound, and sometimes pliable electrodes, quite unlike the weak and friable plain zinc.

The electrodes were cycled under a harsh regime, which accelerated failure by the shedding of active material. Most polymers reduced both the current and the total charge which could be withdrawn from the electrode, notably PS and PVC, apparently by choking the electrode with discharge reaction products. Some polymers could markedly increase the cycle life, however, including PMA, PVA, PI and, notably, PC. The level of addition of the first three materials was critical — too much could choke the electrode PC is the outstanding exception for it did not impede the electrode reaction, even at high levels of addition It also stabilised the deposit formed during charging, thus reducing shedding and increasing cycle life. The cycling performance of the polymeric electrode materials can be related to their steady state polarisation behaviour.

These results show that the very severe cycling test described here can provide a means of rapidly assessing polymeric binders for secondary zinc electrodes. The severity of the test resulted in very short cycle lives However, the pattern of results may be expected to be repeated on a longer time scale with practical systems. Further work is in progress.

Acknowledgements

We would like to thank Dr. M C. Ball for electron microscopy and helpful discussion of electrode structures. We are grateful for financial support from SERC (A.J.S.M.).

References

1 R W Powers, *J Electrochem Soc*, *116* (1969) 1652
2 R W Powers, *J Electrochem Soc*, *118* (1971) 685
3 R W Powers and M W Breiter, *J Electrochem Soc*, *116* (1969) 719
4 M W Breiter, *Electrochim Acta*, *16* (1971) 1169
5 M C H McKubre and D D Macdonald, *J Electrochem Soc*, *128* (1981) 524
6 M B Liu, G M Cook and N P Yao, *J Electrochem Soc*, *128* (1981) 1663
7 N A Hampson, M J Tarbox, J T Lilley and J P G Farr, *Electrochem Technol*, *2* (1964) 309
8 N A Hampson and M J Tarbox, *J Electrochem Soc*, *110* (1963) 95
9 R N Elsdale, N A Hampson, P C Jones and A N Strachan, *J Appl Electrochem*, *1* (1971) 213
10 G Coates, N A Hampson, A Marshall and D F Porter, *J Appl Electrochem*, *4* (1974) 75
11 M W Breiter, *Electrochim Acta*, *15* (1970) 1297
12 J Turner and P F Hutchison, *Power Sources*, *6* (1977) 335
13 Z Nagy and J O'M Bockris, *J Electrochem Soc*, *119* (1972) 1129
14 S Szpak and C J Gabriel, *J Electrochem Soc*, *126* (1979) 1914
15 T Katan, J R Savory and J Perkins, *J Electrochem Soc*, *126* (1979) 1835
16 A Marshall and N A Hampson, *J Appl Electrochem*, *7* (1977) 271
17 J McBreen, *J Electrochem Soc*, *119* (1972) 1620
18 J McBreen and E J Cairns, *Adv Electrochem Electrochem Eng*, *11* (1978) 273
19 S Szpak, C J Gabriel and T Katan, *J Electrochem Soc*, *127* (1980) 1063
20 K W Choi and D N Bennion, *J Electrochem Soc*, *123* (1976) 1616
21 K W Choi, D Hamby and D N Bennion, *J Electrochem Soc*, *123* (1976) 1628
22 W G Sunu and D N Bennion, *J Electrochem Soc*, *127* (1980) 2007
23 W G Sunu and D N Bennion, *J Electrochem Soc*, *127* (1980) 2017
24 Y Yamazaki and N P Yao, *J Electrochem Soc*, *128* (1981) 1655
25 Y Yamazaki and N P Yao, *J Electrochem Soc*, *128* (1981) 1658
26 D C Hamby and J Wirkkala, *J Electrochem Soc*, *125* (1978) 1020
27 D C Hamby, N J Hoover, J Wirkkala and D Zahnle, *J Electrochem Soc*, *126* (1979) 2110
28 M B Liu, G M Cook and N P Yao, *J Electrochem Soc*, *129* (1982) 239
29 G A Dalin, in A Fleischer and J J Lander (eds), *Zinc–Silver Oxide Batteries*, Wiley, New York, 1971, p 87
30 S P Poa and S J Lee, *J Appl Electrochem*, *9* (1979) 307
31 A Charkey, *26th Power Sources Symp*, 1974, p 87
32 A Charkey, *Power Sources*, *4* (1972) 93
33 M Cenek, O Kouřil, J Šandera, A Toušková and N Calábak, *Power Sources*, *6* (1977) 215
34 R Holze and A Maas, *J Appl Electrochem*, *13* (1983) 549
35 S Kulcsár, J Áagh, Á Fazekas, J Vigh and Z Bujdoso, *J Power Sources*, *8* (1982) 55
36 M H Katz, J T Nichols, F R McLarnon and E J Cairns, *J Power Sources*, *10* (1983) 149
37 N A Hampson and A J S McNeil, *J Power Sources*, *15* (1985) 245
38 A J S McNeil and N A Hampson, *Surf Technol*, *19* (1983) 335
39 D P Gregory, P C Jones and D P Redfearn, *J Electrochem Soc*, *119* (1972) 1288
40 T S Chang, Y Y Wang and C C Wan, *J Power Sources*, *10* (1983) 167
41 J O'M Bockris, Z Nagy and A Damjanovic, *J Electrochem Soc*, *119* (1972) 285